JOURNAL OF PROPULSION AND POWER
Vol. 11, No. 1, January–February 1995

Structure of Coal Water Slurry Sprays

Manikandan Prithiviraj* and Malcolm J. Andrews†
Texas A&M University, College Station, Texas 77840

A model of coal water slurry (CWS) sprays is presented with new experimental data for CWS viscosities and surface tension. The model is based on the aerodynamic theory of spray atomization that has been successfully used for diesel sprays. However, the higher CWS viscosity makes their behavior different from diesel sprays. For comparison with experiment the following spray parameters are identified; spray angle, intact core length, drop diameters, and velocities of drops and gas. The results from the computations have been compared with experimental measurements reported in the literature. Computed spray angles and penetration rates agree well with experimental measurements. Computed drop sizes show the right trend when the injection pressure and the axial location at which the Sauter mean diameter is measured are varied.

Nomenclature

A = function in Taylor's analysis
A_θ = constant of the initial spray angle
B = function in Taylor's analysis
B_d = constant of the initial drop size equation
C, C_c = constants of the intact core length
C_d = coefficient of discharge of the nozzle
D_n = nozzle diameter
d_0 = initial drop diameter calculated from Eq. (2)
f_m^* = dimensionless frequency of fastest growing wave
Im = imaginary part
k = wave number
L = length of the nozzle
P_a = ambient gas pressure
Re = real part
S = spray tip penetration distance
s = real part of nondimensional temporal growth rate
Ta = Taylor number $\rho_l\sigma^2/\rho_g\mu_l^2V_T^2$
t = time
t_b = breakup time
U = average axial centerline velocity of drops/gas
U_0 = average injection velocity
u' = axial perturbation velocity of the CWS jet
V_{inj} = ideal injection velocity
V_T = relative velocity between the liquid and gas
v' = radial perturbation velocity of the CWS jet
X_1 = length of the CWS spray intact liquid core
x = axial distance
y = radial distance
α = temporal growth rate of the CWS velocity perturbation
$\dot{\gamma}$ = shear rate
ΔP = instantaneous injection pressure
ΔP_{avg} = average injection pressure
η = surface elevation of the CWS velocity perturbation
η_b = surface elevation of CWS velocity perturbation at breakup
θ = initial angle of the CWS spray
λ_m = wavelength of the fastest growing wave
λ_m^* = dimensionless wavelength of fastest growing wave
μ_l = dynamic viscosity of CWS
ν = kinematic viscosity of CWS
ρ_g = density of gas
ρ_l = density of CWS
σ = surface tension of CWS
ϕ = velocity potential from Taylor's analysis
ϕ' = velocity potential of perturbation from Taylor's analysis
ω_m = growth rate of the fastest growing wave
ω_m^* = dimensionless growth rate of fastest growing wave

Received Sept. 30, 1993; revision received April 30, 1994; accepted for publication May 10, 1994.
*Graduate Student.
†Assistant Professor.

Introduction

THE use of coal water slurry (CWS) as an alternative to diesel fuel in compression ignition engines has emerged in recent years for conserving our oil reserves.[1] The efficiency and emissions of an engine are strongly affected by the combustion process, which is strongly dependent on the spray structure and characteristics. Experimentation on CWS sprays has produced data on spray angles, liquid core lengths, drop diameters, and velocity profiles. Modeling of the sprays and comparison of the model with data forms a firm foundation for understanding the spray structure and characteristics, which can then be used for design purposes. Phatak and Gurney[2] reported an early experimental study that included work to characterize a slurry spray. They obtained partial data on the droplet size distribution from an air blast injector. Nelson et al.[3] obtained a drop size distribution for CWS sprays. Yu et al.[4] studied the effects of fuel type, nozzle geometry, and injection pressures on the transient CWS sprays. Seshadri[5] and Caton et al.[6] conducted several tests measuring spray angles and penetration rates. Kihm et al.[7] studied the effect of axial location, injection pressure, and ambient density on the Sauter Mean Diameter (SMD) of drops at the tip of the CWS spray. Modeling of CWS sprays has received limited attention, and to the authors' knowledge this work is one of the first attempts. A detailed literature review can be found in Prithiviraj.[8]

Atomized sprays are obtained by the injection of a high-velocity fluid into a compressed gas. Aerodynamic interaction between the gas and the fluid causes the breakup of the jet close to the nozzle exit. Figure 1 shows the structure of an atomizing spray with the virtual origin or the point from which all the momentum of the spray apparently originates, the length of an intact liquid core of injected fluid that extends from the nozzle exit, and the end of the developing region. The spray has reached its steady-state configuration at the end of the developing region and resembles a turbulent incompressible jet. This article concentrates on the atomization caused by injection of a liquid into a compressed gas since this is the typical atomization mode in CWS fueled engines. This aerodynamic atomization may be contrasted with two-

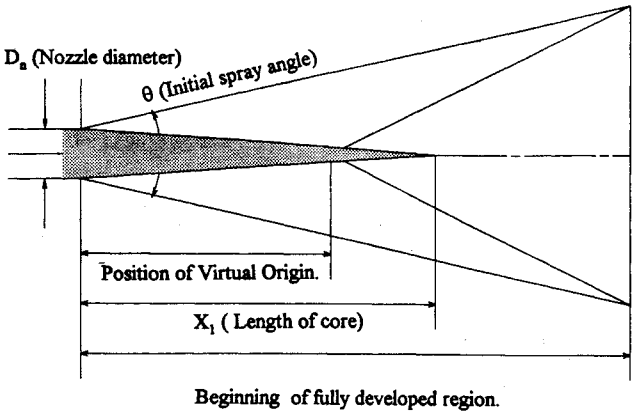

Fig. 1 Structure of a high-speed atomizing spray.

fluid atomization, which uses a gas having a high kinetic energy to disintegrate the liquid.

The successful aerodynamic theory of jet breakup[9] for diesel spray atomization is based on the pioneering work of Taylor.[10] Since the present work uses some of Taylor's results and largely extends the work of Reitz and Bracco,[9] the next section reviews these works. This is followed by modifications in the analysis to account for the higher viscosity of the CWS sprays. The solution of the model partial differential equations is described. Results from the numerical solutions are then compared with the experimental results of Seshadri,[5] Caton et al.,[6] and Kihm et al.[7] These experiments represent a complete set of data that are sufficient to validate our model. This article closes with conclusions drawn from this work.

Background

Taylor[10] analyzed the breakup of a viscous, flat liquid surface due to the action of wind blowing over the surface. He assumed that ripples are produced by an agency exerting normal pressure, but no tangential stress at the liquid surface. He did a linear stability analysis and deduced the frequency, wavelengths, and growth rates of the perturbations. He reasoned that the fastest growing wave causes the liquid surface breakup.

Reitz and Bracco[9] conducted several experiments on atomizing diesel sprays and considered the effect of nozzle geometry in the breakup process. Their diesel spray experiments determined the constants in Taylor's[10] equations for θ, d_0 (which is the diameter of the drops ejected from the core), and X_1, that extends from the nozzle outlet. These equations are:

$$\tan(\theta/2) = (1/A_\theta)4\pi(\rho_l/\rho_g)^{1/2}f_m^* \quad (1)$$

$$d_0 = B_d(2\pi\sigma/\rho_g V_T^2)\lambda_m^* \quad (2)$$

$$(X_1/D_n) = C_c f_m^{*-1}(\rho_l/\rho_g)^{1/2} \quad (3)$$

Where the parameters λ_m^* and ω_m^* are given as

$$\lambda_m^* = \left(\frac{\rho_g V_T^2 \lambda_m}{2\pi\sigma}\right)$$
$$\omega_m^* = \tfrac{1}{2}\sqrt{(\rho_l/\rho_g)}(\sigma/\rho_g V_T^3)\omega_m \quad (4)$$

These equations and the parameters therein need some explanation. Figure 1 shows the definition of the initial full angle of the spray θ. Equation (1) is the ratio of radial and axial velocities of the most unstable wavelengths presumed to form drops. A_θ is an experimentally determined function that depends on the nozzle geometry and is given by Reitz and Bracco[9] as

$$A_\theta = 3 + 0.28(L/D_n) \quad (5)$$

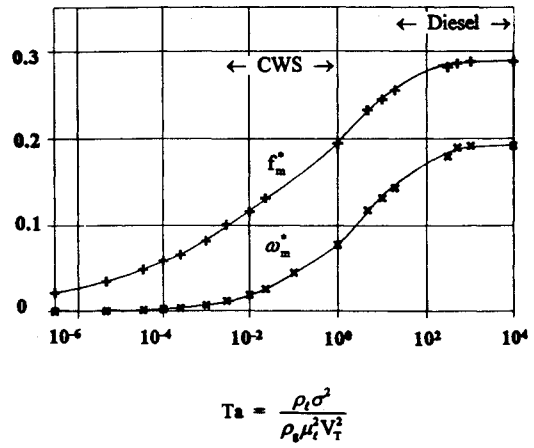

Fig. 2 Stability analysis functions from Taylor.

The parameter f_m^* is a nondimensional number that is the product of the nondimensional growth rate ω_m^*, and the nondimensional wavelength λ_m^* of the fastest growing (most unstable) wave. Taylor[10] provided an evaluation of f_m^*, ω_m^*, and λ_m^* that are functions of Ta. Figure 2 shows the variation of f_m^* and ω_m^* with Ta. f_m^*, ω_m^*, and λ_m^* take asymptotic constant values for diesel sprays.[11]

Equation (2) gives d_0, the diameter of the drops as they are ejected from the liquid core. The assumption is made that the diameter of drops ejected from the liquid core is proportional to the wavelength of the fastest growing wave at the time of breakup, where B_d is a constant that is found from experimental data. V_T is the velocity of the liquid surface relative to the gas. Chatwani and Bracco[12] recommended a value of one-fourth of the ideal injection velocity since this value gave a realistic initial drop size for diesel sprays. The drop diameter computed from Eq. (2) is appropriate only near the nozzle exit. Drop collisions, breakup, and coalescence cause a distribution of drop sizes as the spray continues downstream in the model.

Equation (3) gives the core length nondimensionalized with respect to the nozzle diameter. In the aerodynamic theory of jet breakup for diesel sprays, $C_c f_m^{*-1}$ is a constant C, which takes a value of 7.0 for diesel sprays.[13]

Experimental Measurements of CWS Viscosities and Surface Tension

Figure 2 shows that the full spray angle, drop diameter, and core length depends on f_m^*, λ_m^*, and ω_m^*, which are functions of Ta. The viscosity and the surface tension of the CWS are required to compute Ta, and so our measurements are described next. The CWS used by Caton et al.[6] had constituents of 82.59% carbon, 5.34% hydrogen, 2.08% nitrogen, 0.18% chlorine, 1.01% sulfur, and 7.58% oxygen. The mean particle diameter of the coal particles in the CWS was 3 μ.

Viscosity Measurements

The viscosity of CWS shows widely varying trends.[14] Our CWS atomization model is based on extensive experimental data collected by Caton et al.[6] However, these data did not include viscosity measurements, and so a viscosity determination at various coal loadings was done for CWS obtained from Caton.

A FANN 35 Couette viscometer was used for the measurements. The viscometer was calibrated using silicone oil. Figure 3 shows the variations of viscosity with shear rate for our CWS and for coal loadings of 46.7, 42.9, 33.5, and 21.3%. The coal loading refers to the ratio of the mass of coal to the total mass (mass of water + mass of coal). For comparison, the coal loading of the CWS used in the GE test engine by Hsu et al.[1] was 50%. Figure 3 shows that the viscosity increases with coal loading and decreases with shear rate for

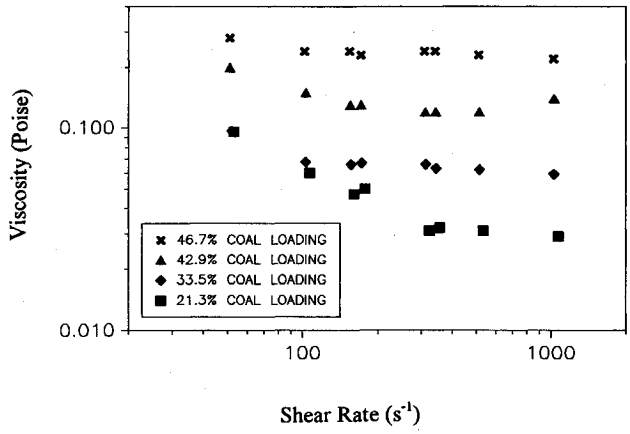

Fig. 3 Measured viscosity for various CWS samples.

the CWS of Caton. It is apparent from Fig. 3 that the viscosity attains a limiting value at high shear rates. Experimental equipment limitations prevented measurements for shear rates greater than 1020 s^{-1}.

Surface Tension Measurement

A FISHER Surface Tensiometer Model 20 measured the surface tension of the CWS sample used by Caton et al.[6] The instrument was calibrated using distilled water. The surface tension of a CWS sample having a coal loading of 50% was measured to be 0.0395 N/m. The surface tension of our CWS is less than the surface tension of water due to the presence of surfactants.

Theoretical Analysis

Shear rates involved in atomizing CWS sprays have been determined using the results of Taylor's[10] linear stability analysis, for purposes of finding the shear rate at which the viscosity should be taken for the atomization mode. This approach recognizes that the shear rate for a small perturbation of the surface of the liquid core depends on the growth rate of the perturbation and its wavelength. Following the analysis of Taylor,[10] formulas for η, ϕ, and k are

$$\eta = -[kA/(\alpha + 2\nu k^2)]e^{(ikx+\alpha t)} \tag{6}$$

$$\phi = -V_T x + \phi' \tag{7}$$

with

$$\phi' = B\exp(-ky + ikx + \alpha t), \qquad k = (2\pi/\lambda_m) \tag{8}$$

The assumption is the perturbation wavelength and amplitude are much smaller than the diameter of the liquid jet so that jet curvature can be neglected. The functions A and B have been found from relationships given by Taylor[10] as

$$\begin{aligned} A &= -[\eta(\alpha + 2\nu k^2)/ke^{(ikx+\alpha t)}] \\ B &= (\eta/k)(\alpha + iV_T k)e^{(-ikx-\alpha t)} \end{aligned} \tag{9}$$

From Taylor's[10] velocity potential, we computed the shear rates $\dot{\gamma}_{xy}$, $\dot{\gamma}_{xx}$, and $\dot{\gamma}_{yy}$. For example

$$\dot{\gamma}_{xy} = \frac{\partial u'}{\partial y} = \frac{\partial}{\partial y}\left(-\frac{\partial \phi'}{\partial x}\right) \tag{10}$$

After inserting Eqs. (7) and (9) into Eq. (10), and some lengthy algebra, we get the following equation for the shear rate $\dot{\gamma}_{xy}$:

$$\begin{aligned} \dot{\gamma}_{xy} &= ik\eta(\alpha + iV_T k)e^{-ky} \\ \dot{\gamma}_{xx} &= -\dot{\gamma}_{yy} = k\eta(\alpha + iV_T k)e^{-ky} \end{aligned} \tag{11}$$

The real part of the shear rate can be obtained from Eq. (11) after some algebraic manipulation as

$$\begin{aligned} Re(\dot{\gamma}_{xy}) &= k[\mathrm{Re}(\eta)I(\alpha) + \mathrm{Re}(\eta)V_T k + \mathrm{Im}(\eta)\mathrm{Re}(\alpha)]e^{-ky} \\ \mathrm{Re}(\dot{\gamma}_{xx}) &= -\mathrm{Re}(\dot{\gamma}_{yy}) = k[\mathrm{Re}(\eta)\mathrm{Re}(\alpha) \\ &\quad - \mathrm{Im}(\eta)\mathrm{Im}(\alpha) - \mathrm{Im}(\eta)V_T k]e^{-ky} \end{aligned} \tag{12}$$

Where Re denotes the real part and Im denotes the imaginary part of the variable in the parentheses. Taylor[10] found the real and imaginary parts of α given in Eq. (13):

$$\begin{aligned} Re(\alpha) &= \omega_m \\ \mathrm{Im}(\alpha) &= \nu k^2\left\{\frac{-\sqrt{(\rho_g Ta/\rho_l)}s\lambda_m}{1 + s - [(1+2s)^{-1/2}/2] + (\rho_g/\rho_l)s}\right\} \end{aligned} \tag{13}$$

with

$$s = [\mathrm{Re}(\alpha)/2\nu k^2] \tag{14}$$

Equation (4) can compute λ_m.

Bracco[11] noted from Taylor's analysis that the amplitude of the wave at the time of breakup η_b is given as

$$\eta_b = (1/A_\theta)(2\pi\sigma\lambda_m^*/\rho_g V_T^2) \tag{15}$$

Equation (12) uses Eq. (13) to compute the shear rates in the experiments of Seshadri[5] and Caton et al.[6] For example, for test 27 of Seshadri[5] (see Table 1), the break-up time[11] t_b and $\dot{\gamma}_{xy}$ take values of 3.1×10^{-5} s, and 3.39×10^6 s^{-1} respectively. Prithiviraj[8] showed the shear rates from Eq. (12) for the simulated experiments to have values between 6×10^3 and 7×10^7 s^{-1}. The large shear rate at the time of breakup and its large value over the growth of the perturbation[8] show that the atomizing shear rates are much higher than those at which the present viscosity measurements could be taken because of equipment limitations.

Cho and Choi[15] measured the viscosity of four samples of CWS for shear rates between 3–30,000 s^{-1}. Two samples showed a shear thickening behavior and the remaining two samples showed a shear thinning behavior. Cho and Choi[15] and Caton et al.[6] observed that shear thickening CWS clogs the injectors and does not atomize. Therefore, we have concentrated on the shear thinning examples of the Caton et al.[6] CWS.

One of the shear thinning samples of Cho and Choi[15] had a coal loading of 52.5% and a mean particle size of 30 μ. The viscosity of this sample decreased about 4% when the shear rate increased from 15,000–30,000 s^{-1}. The other shear thinning sample had a coal loading of 52% and a mean particle size of 10 μ. The viscosity of this sample remained constant for shear rates between 15,000–30,000 s^{-1}. The Caton et al.[6] CWS had a coal loading between 45–50% and a mean particle size of 3 μ. Thus, given the measured limiting viscosity shown in Fig. 3 and the evidence of Cho and Choi using similar CWS, we have extrapolated an asymptotic constant viscosity value of 0.023 Pa·s for our CWS.

Figure 2 shows that f_m^* and ω_m^* in diesel sprays take asymptotic constant values since the Taylor number is large and it is reasonable to take $C_c f_m^{*-1}$ as a constant in Eq. (3). However, these functions vary with the Taylor number (see Fig. 2) in CWS sprays, and so the full Taylor form of Eq. (3) with $C = C_c f_m^{*-1}$ is required. Table 1 gives values for $C_c f_m^{*-1}$ that range from 9.4 to 12.9, which is 30–50% higher than the 7.0 value used for high-speed diesel sprays.

Thus, Eqs. (1–3) and Fig. 2, together with an asymptotic constant viscosity value and surface tension, form our atomization model of CWS sprays.

Table 1 Results of simulation of CWS sprays from Seshadri[5] (7 and 27) and Caton et al.[6] (1, 2a, 2b, 2c, 2d, 3)

Experimental conditions					Theoretical parameters		Computed results		
Test	D_n, mm	ρ_g, kg/m^3	ΔP, MPa	P_a, MPa	Ta	$C_c f_m^{*-1}$	θ, deg	d_0, μm	(X_1/D_n)
7	0.2	1.2	31.5	0.1	2.4	9.8	1.8	136	311.3
27	0.4	25.0	21.2	2.1	0.17	12.7	6.3	15.1	88.9
1	0.2	25.0	83.0	2.1	0.04	12.7	6.4	5.4	102.7
2a	0.4	25.0	28.0	2.1	0.13	11.6	7.4	12.3	88.9
2b	0.4	25.0	55.0	2.1	0.07	12.6	6.8	7.5	96.3
2c	0.4	25.0	83.0	2.1	0.04	12.9	6.4	5.4	102.7
2d	0.4	25.0	110.0	2.1	0.03	12.8	6.2	4.3	106.7
3	0.2	25.0	83.0	0.1	0.91	9.4	2.0	61.4	338.9

ρ_l = 1200 kg/m^3; σ = 0.0395 N/m; μ_l = 0.023 Pa s; C_c = 1.75.

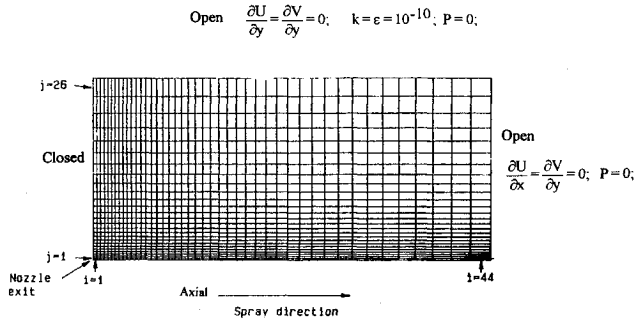

Fig. 4 Computational grid.

Spray Model

The CWS atomization model described above must be tested against experimental data. To this end the atomization model has been incorporated into an Eulerian/Lagrangian formulation for simulation of sprays. The formulation originated from the stochastic parcel method of Dukowicz.[16] O'Rourke[17] later accounted for drop collisions, breakup, coalescence, and evaporation. We neglect evaporation in our computations because the experiments of Seshadri[5] and Caton et al.[6] were conducted at room temperature.

The complete computational model uses a stochastic description of CWS drop motions in the CWS spray with an Eulerian description of the conservation laws governing the mean properties of the gas phase, and a Lagrangian description for parcels of CWS drops. Each parcel represents a group of CWS drops with the same physical properties (size, velocity, and position). Parcels are injected into the computational domain using the line source technique of Chatwani and Bracco[12] to represent the finite core length of the CWS spray. A Monte Carlo technique chooses parcel properties with mean values taken from the CWS spray theory of the last section. The computer program follows the parcels using a Lagrangian calculation that accounts for the effect of drag, drop collisions, and coalescence.[18] The k-ε model[19] represents the gas turbulence. O'Rourke and Bracco[20] give the detailed equations of the Lagrangian/Eulerian formulation.

The computations use an axisymmetric two-dimensional grid shown in Fig. 4. The boundary conditions imposed are 1) open top and right boundaries at the ambient pressure to simulate a spray in a semi-infinite gas, 2) a symmetry line at the center, and 3) a solid free-slip boundary on the left-hand side. These boundary conditions match well with the experimental conditions to be modeled. The grid has 44 cells in the axial direction and 26 cells in the radial direction. The initial cell sizes are 0.2 and 0.05 cm in the axial and radial directions, respectively. A linear expansion factor of 1.06 is employed both in the axial and radial directions. Andrews and Bracco[18] successfully used this computational grid in previous work. Prithiviraj[8] showed the computations to be grid independent.

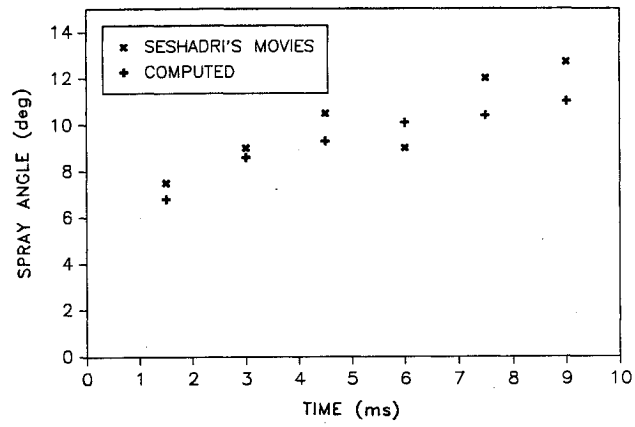

Fig. 5 Variation of spray angle with time for test 27 of Seshadri.[5]

Results and Discussion

Table 1 shows two tests of Seshadri,[5] listed as tests 7 and 27, and six tests of Caton et al.,[6] listed as tests 1, 2a, 2b, 2c, 2d, and 3, but many others can be found in Prithiviraj.[8] Seshadri[5] used a Bendix injector commonly used in medium speed diesel engines. In this injector, the injection pressure varies with time. Caton et al.[6] used a state-of-the-art accumulator injection system that could maintain a constant injection pressure throughout the injection cycle. Seshadri[5] and Caton et al.[6] obtained data on the time-varying spray angle and the penetration rates. Kihm et al.[7] measured the drop SMD for the tests of Caton et al.[6] using a laser diffraction particle analyzing (LDPA) technique. This technique allowed them to measure the SMD of drops near the tip of the spray where the light extinction was low and the data free from multiscattering bias. Table 1 gives the experimental conditions along with the computed initial spray angle, initial average drop diameter, and the intact core length.

Spray Angle

The spray angle is the arc tangent of the spray width divided by the axial distance from the nozzle exit to the measurement location. Seshadri[5] and Caton et al.[6] measured the spray angle at an axial distance of 6 cm from the nozzle exit. This spray angle is different from θ of Eq. (1), and its determination from the simulation is described next.

To compute the spray angle we compute the radial cumulative liquid volume for all cells on the grid situated at a fixed axial distance of 6 cm from the injector. The location of the spray edge is taken to be the location of the outermost radial cell that has a cumulative liquid volume of 99%.

Figures 5 and 6 show the measured and computed values of the time-varying spray angle for test 27 of Seshadri,[5] and test 2c of Caton et al.,[6] respectively. In both figures, the computed spray angle agrees well with the experiments and

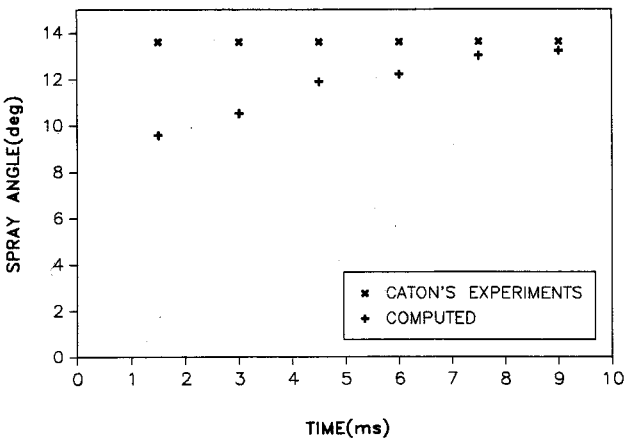

Fig. 6 Spray angle variation for test 2c of Caton et al.[6]

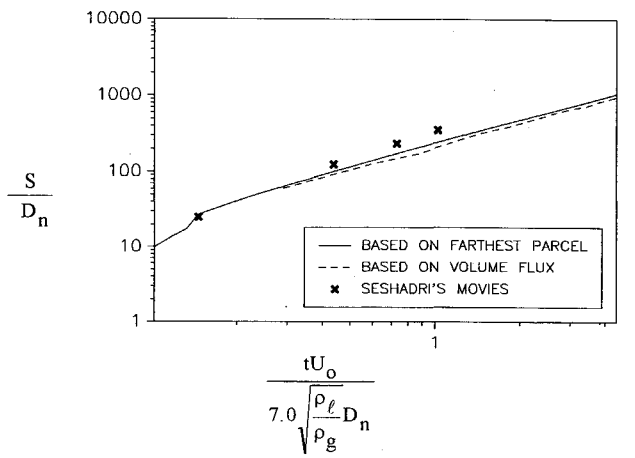

Fig. 7 Comparison of computed spray tip penetration with algebraic formulas and experimental results for test 7 of Seshadri.[5]

increases with time. The gradual turbulent dispersion of drops and gas causes the increasing spray angle. This phenomenon has also been observed in all of Seshadri's CWS diesel engine spray experiments. Caton's experiments do not show this increase in spray angle. A reason for this difference is not readily apparent. However, Fig. 6 shows that the predicted steady-state spray angle for the Caton et al.[6] experiments agree very well with the experimental measurements.

Spray Penetration Rates

Two methods have been used to compute the spray penetration distance from the predictions. The first method assumes the tip of the spray to be the location of the farthest parcel. The second method, referred to as volume flux, assumes the penetration distance to be the axial location before which 95% of the total liquid volume is found when starting from the nozzle. The time in all the spray penetration plots is normalized with respect to the time taken by the spray to travel one liquid core length [based on Eq. (3) with $C_c f_m^{-1} = 7.0$] at the ideal injection velocity. The spray penetration distance is normalized with respect to the nozzle diameter. Figures 7–10 show the penetration computed by taking the farthest parcel as a solid line, by taking the volume flux as a dotted line, and that measured by Seshadri[5] or Caton et al.[6] as crosses.

Figures 7 and 8 show the spray tip penetration computed by the spray code and from the movies of Seshadri[5] for two test cases. Seshadri's experiments used a transient injection pressure so that in the computations an ideal injection velocity

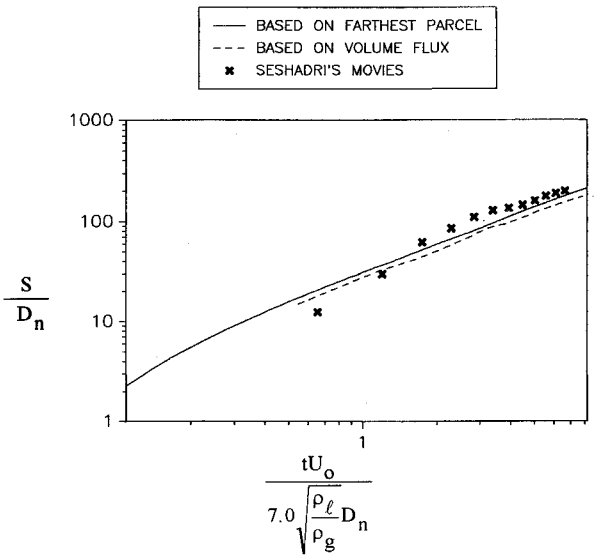

Fig. 8 Comparison of computed spray tip penetration with algebraic formulas and experimental results for test 27 of Seshadri.[5]

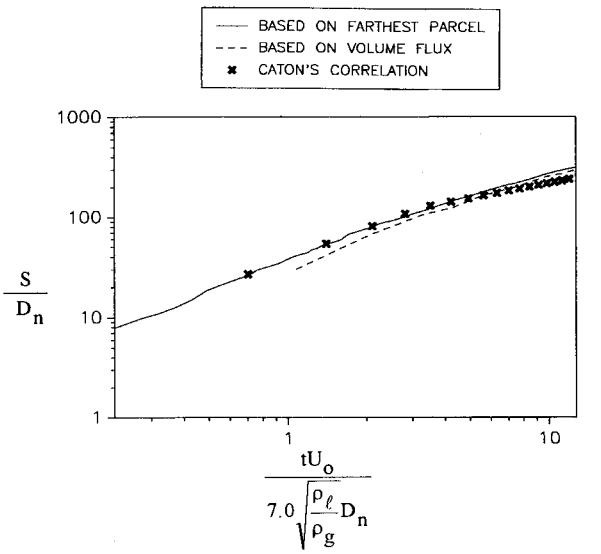

Fig. 9 Comparison of computed spray tip penetration with algebraic formulas and experimental results for test 2c of Caton et al.[6]

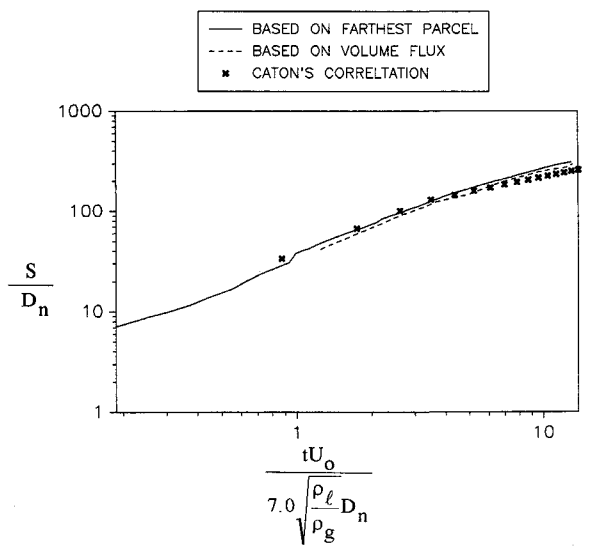

Fig. 10 Comparison of computed spray tip penetration with algebraic formulas and experimental results for test 2d of Caton et al.[6]

computed from experimental injection pressure traces prescribed the spray axial velocity. V_{inj} and U_0 are given as

$$V_{inj} = C_d\sqrt{(2\Delta P/\rho_l)}, \qquad U_0 = C_d\sqrt{(2\Delta P_{avg}/\rho_l)} \quad (16)$$

with $C_d = 0.56$. We have taken ΔP as the instantaneous injection pressure and ΔP_{avg} as the average experimentally measured injection pressure from the start of injection to 1.5 ms. U_0 is used for normalizing the spray parameters in Figs. 7–11. The low value for C_d is consistent with the Reitz[21] observation that liquids with a higher viscosity have a lower C_d. Caton et al.[6] observed that CWS sprays with a coal loading of 50% penetrate about 15% faster than diesel sprays under identical injection conditions. Consequently, we used a velocity of the CWS spray tip as 79.5% of the ideal injection velocity.

Figures 9 and 10 show the spray tip penetration computed by the spray code and that obtained from the experimental correlation of Caton et al.[6] for CWS sprays. The injection velocities used are those given by Eq. (16). V_{inj} and U_0 are equal since the injection pressure was constant in the experiments of Caton et al.[6]

The comparison in Figs. 7 and 8 of the computer simulation with Seshadri's[5] data shows good overall agreement. The discrepancies in the computed penetration rates for tests 7 and 27 may be attributed to difficulties we had identifying the start of injection, and consequently the use of transient injection pressure traces. Figures 9 and 10 show simulations for the Caton et al.[6] experiments. The results compare well with the experiments. Here, the injection pressure is constant, and so it was much easier to compute an accurate injection velocity with Eq. (16). The figures show that the spray initially travels at a constant velocity. This region is usually attributed to the intact liquid core for diesel sprays. After breakup of the liquid core, the spray moves at a slower velocity resulting in a reduced penetration rate shown by the correlations of Caton et al.,[6] and by the change of slope in Figs. 7–10. Prithiviraj[8] observed similar trends in other test cases.

Drop Sauter Mean Diameters

Kihm et al.[7] considered the effect of axial location, injection pressure, and ambient density on the SMD of the drops at the tip of the CWS spray. For comparison purposes we identified the drops at the tip of our spray and recorded their SMD in an identical manner to that of Kihm et al.[7]

Table 2 shows a comparison between the drop SMD computed by the spray code and those measured by Kihm et al.[7] for test 1 of Caton et al.[6] where the axial location varies from 60 to 120 mm. The increase in drop diameter downstream is due to collisions and coalescence. The spray code predicts this trend well. However, the drop size at 60 mm is overestimated. This overprediction might be due to an overestimate of the initial drop size. The average SMD of coal particles in our CWS samples is 3 μm.[6] The minimum drop diameter based on a volumetric balance basis may be calculated to be 4 μm for a coal loading of 50%. Table 1 shows that the lowest value of the computed initial drop diameter is 4.3 μm for test 2d of Caton et al.[6] Prithiviraj[8] confirmed that better estimates

Table 2 Variation of SMD with axial location for test 1 of Table 1

Axial location, mm	SMD, μm	
	Kihm et al.[6]	Present simulations
20	Not measured	20
40	Not measured	35
60	16	43
80	25	52
100	39	64
120	47	75

$D_n = 0.2$ mm; $\Delta P = 83$ MPa; $\rho_g = 25.0$ kg/m^3; $d_0 = 5.4$ μm.

Table 3 Variation of SMD with injection pressure

Test case	Injection pressure, MPa	SMD, μm	
		Kihm et al.[6]	Present simulations
2a	28	92	115
2b	55	68	76
2c	83	50	61
2d	110	32	54

$D_n = 0.4$ mm; $\rho_g = 25.0$ kg/m^3; $X = 120$ mm.

Table 4 Variation of SMD with ambient density

Test case	Ambient density, kg/m^3	SMD, μm	
		Kihm et al.[6]	Present simulations
2c	25	47	75
3	1.2	20	175

$D_n = 0.4$ mm; $\Delta P = 83$ MPa; $X = 120$ mm.

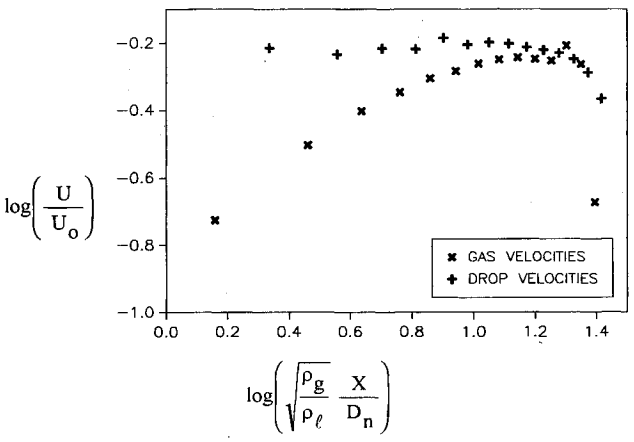

Fig. 11 Comparison of computed average gas and drop centerline velocities for test 27 of Seshadri.[5]

of the SMD could be obtained by using smaller initial drop sizes. However, under some circumstances this may reduce the initial drop size below the minimum permitted value of 4 μm. More initial drop size data is needed for CWS sprays before we can conclude on overestimation of the drop size.

Table 3 shows a comparison between the drop SMD computed by the spray code and those measured by Kihm et al.[6] when the injection pressure varied from 28 to 110 MPa (tests 2a–2d of Caton et al.[6]). The decrease in drop SMD with an increase in injection pressure is due to the faster breakup of drops caused by increased aerodynamic forces at higher injection velocities. The spray code predicts the trend well, but again overpredicts the drop size. This overprediction is consistent with an overestimate of the initial drop size.

Table 4 shows a comparison between the drop SMD computed by the spray code and those measured by Kihm et al.[7] when the ambient gas density was varied (tests 1 and 3 of Caton et al.[5]). A conflicting trend may be observed between the experimental observations and the computations. Several research workers observed various trends in the variation of SMD with ambient density in diesel sprays. For instance, Giffen and Lamb[22] observed an increase in SMD when the ambient density decreases, whereas Hiroyasu and Kadota[23] observed a decrease in SMD when the ambient density decreases. Bracco[11] observed in experiments with diesel sprays that the diameter of the drops decreased with a decrease in the ambient density. He also mentions that the drop diameter, computed using the supplemented aerodynamic theory of spray atomization, increases with a decrease in the ambient density. Kihm et al.[7] observed a decrease in drop SMD at a lower

ambient density. Our computations show an increase in SMD at lower densities. We believe that an increase in computed SMD at a lower ambient density is because of increased collisions and coalescence caused by a smaller spray angle. However, we are unable to explain the discrepancy at this time.

Drop/Gas Velocities

Figure 11 shows the variation of the computed centerline drop and gas velocity with axial distance, 1.5 ms after the start of injection for test 27 of Seshadri.[5] The figure shows that the average drop velocity near the vicinity of the nozzle is lower than the drop injection velocity, because the drops lose momentum as they accelerate the ambient gas. Downstream, momentum transfer from the high-speed drops to the gas increases the mean gas velocity to a maximum at the tip of the liquid CWS core, and thereafter starts decreasing. As this momentum transfer process takes place, the mean drop velocities decrease and gradually equilibrate with the gas velocities. The steady decrease of drop and gas velocity is due to the expansion of the gas jet reducing the gas velocity, and hence, via drag the drop velocities. The precipitous drop-off of drop and gas velocities at the far right of the plots is associated with the tip of the spray. In the far field (beyond the intact liquid core) the gas and the drop velocities have equilibrated through drag. Consequently, small drops, large drops, and gas have the same velocity as seen in Fig. 11. We infer that a correct prediction of the penetration implies that the drop and gas velocities are being reasonably calculated. The computations of the other test cases[8] show similar behavior.

Conclusions

A stability analysis has shown that high shear rates are present during CWS atomization. The viscosity of our CWS sprays takes an asymptotic constant value at these high shear rates. Consequently, these CWS sprays have been simulated using a model based on an aerodynamic theory of spray atomization, using the full Taylor expression for liquid core breakup length, an asymptotic constant viscosity, and measured surface tension. Use of accurately measured injection pressures were crucial in predicting the injection velocities that permitted our successful calculations. The spray tip penetrations and the spray angles obtained from our simulations agree well with the experimental measurements. Our computational model predicted well the change in slope of the penetration rate due to the breakup of the intact liquid CWS core, which indicates that we correctly computed the length of the intact liquid core. The trend in variation of drop SMD with axial location and injection pressure is well-predicted. We overpredicted drop SMDs, but it is encouraging that our model captured the right physical trends when the injection pressure and the axial location at which the drop sizes are measured are varied. Future experimental data about drop sizes close to the nozzle exit will help resolve the overprediction of drop sizes. Detailed experimental data for gas/drop velocities for the present CWS sprays is not available for comparison. However, agreement of experimental and computed tip penetration rates suggests that the mean drop velocities are being reasonably well-calculated.

We have found that the high shear rates in the atomization process place our non-Newtonian CWS in a region of constant viscosity that results in Newtonian effects. As a result, the aerodynamic theory of jet breakup, originally devised for diesel sprays, has been successfully applied to CWS with two modifications:

1) The intact liquid core length formula (3) with the functional dependencies in Fig. 2 must be used as CWS sprays operate at $Ta < 1$.

2) For our CWS, viscosities should take their high asymptotic shear rate values.

With the recognition that our CWS obeys modified diesel spray-type relations, and the successful comparison of these relations with experimental data, we conclude that Eqs. (1–3) may be employed with (1) and (2) above to describe the CWS spray angle and intact core length. Although the drop SMD computed by the spray code does not accurately compare with the measured data, they predict the right trend, and this is encouraging. We suspect our initial drop size shed from the liquid core may be too large. However, experimental measurements are difficult in this dense spray region, and at present no data close to the nozzle is now available to confirm our suspicion.

Acknowledgments

An Engineering Excellence Grant from the Department of Mechanical Engineering at Texas A&M University, College Station, Texas, supported this work. We thank R. Darby, Department of Chemical Engineering, Texas A&M University, College Station, Texas, for allowing us to use his viscometer for our viscosity measurements and to J. Caton, Department of Mechanical Engineering, Texas A&M University for providing CWS samples for these viscosity measurements. We thank R. Flummerfelt, Department of Chemical Engineering, Texas A&M University, for permitting us to take surface tension measurements in his laboratory.

References

[1]Hsu, B. D., "Coal Fueled Diesel Engine Development Update at GE Transportation Systems in Coal Fueled Diesel Engines," American Society of Mechanical Engineers, Vol. 16, ICE, 1992, pp. 39–46.

[2]Phatak, R. G., and Gurney, M. D., "Investigation of Diesel Fuel Injection Equipment Response to Coal Slurry Fuels," American Society of Mechanical Engineers Paper 85-DGP-17, Feb. 1985.

[3]Nelson, L. P., Seeker, W. R., and Zimpermand, R. A., "The Atomization, Ignition and Combustion Characteristics of Coal Slurry Fuels in Medium Speed Diesel Engines," *Joint Central and Western States Sections*, Combustion Inst., Paper 31A, Pittsburgh, PA, 1985.

[4]Yu, T. U., Lai, M. C., and Beer, J. M., "Injection and Atomization of Coal Water Slurry in High Pressure Diesel Environment in Coal Fueled Diesel Engines," *Journal of the Institute of Energy*, Vol. 64, No. 458, 1989, pp. 12–20.

[5]Seshadri, A. K., "Characterization of Coal Water Slurry Sprays from a Positive Displacement Fuel Injection System," M.S. Thesis, Dept. of Mechanical Engineering, Texas A&M Univ., College Station, TX, 1991.

[6]Caton, J. A., Payne, S. E., Kihm, K. D., and Terracina, D. P., "Coal Water Slurry Spray Characteristics of an Electronically-Controlled Accumulator Fuel Injection System," *Coal Fueled Diesel Engines*, Internal Combustion Engine Div. 19, ASME 1993, pp. 25–32.

[7]Kihm, K. D., Terracina, D. P., Caton, J. A., and Payne, S. E., "Synchronized Droplet Size Measurements for Coal Water Slurry (CWS) Diesel Sprays of an Electronically Controlled Fuel Injection System," *Coal Fueled Diesel Engines*, ICE 19, ASME 1993, pp. 33–42.

[8]Prithiviraj, M., "Modeling the Structure of Coal Water Slurry (CWS) Sprays," M.S. Thesis, Dept. of Mechanical Engineering, Texas A&M Univ., College Station, TX, 1993.

[9]Reitz, R. D., and Bracco, F. V., "Mechanism of Atomization of a Liquid Jet," *Physics of Fluids*, Vol. 25, No. 10, 1982, pp. 1730–1739.

[10]Taylor, G. I., "Generation of Ripples by Wind Blowing over a Viscous Fluid," *Collected Works of G. I. Taylor*, Cambridge Univ. Press, London, 1958.

[11]Bracco, F. V., "Modeling of Engine Sprays," Society of Automotive Engineers Paper 850394, Feb. 1985.

[12]Chatwani, A. U., and Bracco, F. V., "Computation of Dense Spray Jets," International Conf. on Liquid Atomization and Spray Systems (ICLASS-85), Paper 1B/1/1, Feb. 1985.

[13]Chehroudi, B., and Bracco, F. V., "On the Intact Core of Full Cone Sprays," Society of Automotive Engineers Paper 850126, Feb. 1985.

[14]Kihm, K. D., and Caton, J. A., "Apparent Viscosity of Coal Water Slurry Fuels," Combustion and Fuels Research Lab., Dept. of Mechanical Engineering, Texas A&M Univ., Rept. CF-91-03, College Station, TX, 1991.

[15]Cho, Y. I., and Choi, U. S., "Experimental Study of Micronized Coal/Water Slurry Rheology at High Shear Rates," *Journal of Energy Resources Technology*, Vol. 112, No. 1, 1990, pp. 36–40.

[16]Dukowicz, J. K., "A Particle Fluid Numerical Model for Liquid Sprays," *Journal of Computational Physics*, Vol. 35, No. 2, 1980, pp. 229–253.

[17]O'Rourke, P. J., "Collective Drop Effects on Vaporizing Liquid Sprays," Ph.D. Dissertation, Dept. of Mechanical and Aerospace Engineering, Princeton Univ., 1532-T, Princeton, NJ, 1980.

[18]Launder, B. E., and Spalding, D. B., *Mathematical Models in Turbulence*, Academic Press, London, 1972.

[19]O'Rourke, P. J., and Bracco, F. V., "Modeling of Drop Interactions in Thick Sprays and a Comparison with Experiments," *The Institution of Mechanical Engineers, Publication 1980-9*, Paper C404/80, 1980, pp. 101–116.

[20]Andrews, M. J., and Bracco, F. V., "On the Structure of Turbulent Dense Spray Jets," *Encyclopedia of Fluid Mechanics, Vol. 3*, Gulf Publishing, Houston, TX, 1988, pp. 1063–1089.

[21]Reitz, R. D., "Atomization and Other Breakup Regimes of a Liquid Jet," Ph.D. Dissertation, Dept. of Mechanical and Aerospace Engineering, Princeton Univ., 1375-T, Princeton, NJ, 1978.

[22]Giffen, E., and Lamb, T. A. J., "The Effect of Air Density on Spray Atomization," Motor Industry Research Association Rept., 1953/5, 1953.

[23]Hiroyasu, H., and Kadota, T., "Fuel Droplet Size Distribution in a Diesel Combustion Chamber," Society of Automotive Engineers Paper 74017, Feb. 1974.